Numerical Comparison of Mono-static and Multi-static Array Performance in Personnel Screening Systems

Vladimir V. Razevig, Margarita A. Chizh, Valery V. Chapursky, Sergey I. Ivashov, and Andrey V. Zhuravlev
Remote Sensing Laboratory, Bauman Moscow State Technical University
5, 2nd Baumanskaya Str., Moscow 105005, Russia

Abstract— The comparison of the modern microwave screening systems is given in this paper in the aspect of employing mono-static or multi-static antenna configuration, with their numerical models described and applied in the presented numerical experiments. The phenomenological model of scattering from human body and foreign objects is used to obtain the radar signal, which is processed according to the given mono-static or multi-static signal processing algorithms. The model of scattering objects is based on point scatterer approximation of their surfaces. The numerical simulations are performed for human body and foreign objects to obtain detailed radar images for mono-static and two multi-static antenna configurations at a single and multiple frequencies. According to the results of numerical simulations, the same quality of radar images, visually assessed by achievable plan view resolution and the level of artifacts, can be obtained by significantly lesser number of antenna elements in the case of multi-static antenna configuration. It was shown that extending the frequency band from 10 to 16 GHz substantially increases the contrast of the foreign objects placed over the human body.

1. INTRODUCTION

Microwave personnel screening systems are currently being used for the detection of concealed objects on human bodies [1], they are widely deployed in international airports around the world. Up to date, the most widely used system with over 1200 deployments around the world, L-3 ProVision [2], uses two vertical linear antenna arrays and mechanical scanning to form a cylindrical aperture. The system uses dense linear antenna arrays each having 384 antenna elements that provide dense sampling at a fraction of a wavelength [3]. This system is designed in a shape of a transparent portal to isolate movable antenna arrays. Among prospective improvements of this system, which do not change the concept of mechanical scanning around the subject, are: the detection software [2] and reduction in the number of antenna elements by employing multi-static sparse antenna arrays [3]. The last modification is not expected to influence the quality of the radar images generated by the system, but rather intended to reduce the complexity of the system and relevant production costs.

In the multi-static radar [3–5] with sparse antenna arrays that acts as a Multiple Input-Multiple Output (MIMO) system the number of samples of complex amplitude equals to the product of N_T transmitting elements by N_R receiving elements. This follows from the operation principle of the system in which each sample stems from each transmitter-receiver pair. In an antenna array with mono-static antenna elements the number of samples equals the number of mono-static antennas (transceivers) N_{TR}. The total number of antenna elements equals $N_T + N_R$ in the multi-static case and N_{TR} in the mono-static case. It follows that the same number of samples may be acquired by fewer antenna elements if one employs a MIMO antenna array. Thus, the problem of decreasing the number of antenna elements may be treated as the problem of MIMO antenna array synthesis when one needs to get the best resolution in the generated radar image by the minimal number of spatially distributed antennas.

In [6, 7] it was shown, by the example of a 3D object consisting from 13 distributed point scatterers forming a 3D cross, that the resolution of radar images with the multi-static processing technique was not worse (the range resolution was in some cases better) than with the mono-static processing technique and antenna array with densely spaced transceivers. In [3] the letters formed by point scatterers were considered. These simulations can not be regarded as complete because the real volumetric objects such as concealed objects on the human body have a solid (continuous) surface. For such objects, corresponding electrodynamic or phenomenological approximations should be applied [8].

To compare how reduction in the number of antenna elements in a MIMO-based personnel screening system influences the quality of obtained radar images in comparison with the mono-static-based system, the following numerical experiments were performed.

2. ANTENNA CONFIGURATION AND SCANNING METHODS

For the simulation of the mono-static case, a vertical linear antenna array composed of equidistant transceivers was considered. The samples along the horizontal axis were supposed to be acquired by moving this antenna array in the same direction. The sampling intervals and the numbers of samples along each axis were given as follows: $\Delta x = 1\,\text{cm}$, $N_x = 130$, $\Delta y = 1\,\text{cm}$, $N_y = 130$. The equivalent scan area had dimension 129 by 129 centimeters.

The multi-static configuration included two vertically oriented linear antenna arrays consisting of $N_T = 8$ transmitters and $N_R = 16$ receivers. The distances between the adjacent antenna elements in the transmitting array and the receiving array were $\Delta y_T = 2.48\,\text{cm}$ and $\Delta y_R = 8.68\,\text{cm}$ correspondingly. The distance between antenna arrays was $\Delta x_{TR} = 9\,\text{cm}$ (along axis X). The number of transmitting and receiving elements was chosen to give the total number of samples $N_T N_R = 128$ that matches well the number of samples selected for the mono-static case outlined above ($N_y = 130$). The sampling was done by the translational motion of the antenna array in the direction of axis X with the sampling interval $\Delta x = 1\,\text{cm}$ resulting in $N_x = 130$ samples along axis X for each receiving antenna element. The diagram of the antenna configuration for this case is given in Fig. 1.

The scan areas for mono-static and multi-static methods were approximately the same and equaled $129 \times 130.2\,\text{cm}$.

3. PHENOMENOLOGICAL MODEL OF THE OBJECTS AND THE RECONSTRUCTION ALGORITHMS OF MICROWAVE HOLOGRAMS

Modeling of electromagnetic scattering by complex 3D-objects can be based on both electrodynamic and phenomenological models of reflection and diffraction [8]. Phenomenological models are simpler than electrodynamic ones. They approximate the object surface by a set of point scatterers [8], where each point scatterer may have its own local radiation pattern with regard to the local normal. In this paper every modeled objects was considered as a surface given on the rectangular grid with 2-mm steps between its nodes belonging to the plane XOY. The calculation of the reflected field was based on the first-order scattering model, which did not take into account multiple reflections and mutual interference of point scatterers, each of them having the omni-directional scattering diagram.

The 3D-models of scattering objects were created with Autodesk 3DS Max and exported to the STL-format (STereoLitorgaphy) resulting in the approximation of the object surface by triangle facets. The set of the point scatterers for the exported surface was formed by projecting the rectangular grid of equally spaced nodes belonging to XOY plane along axis Z on the object surface. The scatterers located on the shadow side of the object were removed from the initial set and were not considered in the simulation.

Microwave holograms were calculated for the following cases: 1) single-frequency holograms at the frequency $f = 10\,\text{GHz}$; 2) wide-band hologram at six frequencies regularly distributed in 10–16 GHz range.

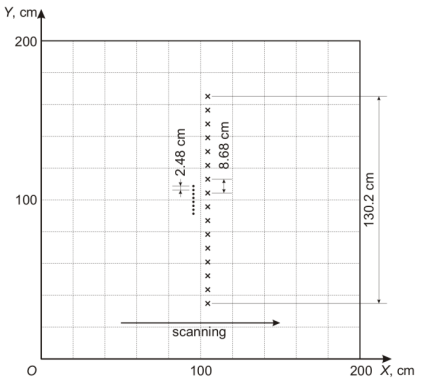

Figure 1: Multi-static antenna configuration.

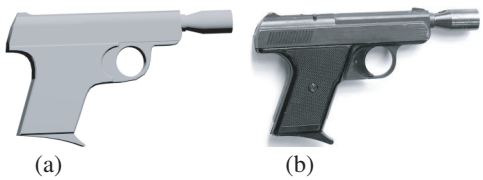

Figure 2: Gas pistol. (a) 3D-model, (b) photo.

3.1. Mono-static Signal Processing

The complex value of the received signal at the frequency f in the scan surface point $(x, y, 0)$ was calculated by

$$E(x,y,f) = \sum_{j=1}^{N_{PS}} \left[g^2\left(f, \theta_j\left(x,y\right)\right) \cdot e^{2i\cdot k\cdot|\mathbf{r}_{x,y}-\mathbf{r}_j|} \right],$$

where N_{PS} is the number of point scatterers in the object model; $k = 2\pi f/c$ is the wavenumber; c is the speed of light; $\theta_j(x,y) = \text{arctg}(\sqrt{(x-x_j)^2+(y-y_j)^2}/z_j)$ is the angle between the normal to the scan surface and the direction from the transceiver element with the coordinate (x, y) toward the scatterer j; $\mathbf{r}_{x,y} = \|x, y, 0\|^T$ is the coordinate vector of the transceiver; $\mathbf{r}_j = \|x_j, y_j, z_j\|^T$ is the coordinate vector of the scatterer j; $|\mathbf{r}|$ is the length of the vector $\mathbf{r}$, $g(f, \theta_j)$ is the radiation pattern of a transceiver element that corresponds to a circular waveguide opening [9]:

$$g(f,\theta) = (1+\cos\theta)\,\frac{J_1\left(k\cdot a\cdot\sin\theta\right)}{k\cdot a\cdot\sin\theta},$$

where a is the radius of the waveguide, $J_1(\xi)$ is the Bessel function of the first kind.

Reconstruction algorithms for the single-frequency and wide-band radar signals (microwave holograms) were given in details in [4, 10].

3.2. Multi-static Signal Processing

The transmitting elements in the MIMO antenna configurations operate sequentially. They emit stepped FM signals in non-overlapping time windows [9]. A multi-static wide-band hologram (the signal registered by the receiving element m while the transmitting element n is operating, when coordinate x of antenna element is x_a) can be expressed as

$$E(n,m,x_a,f) = \sum_{j=1}^{N_{PS}} \left[g\left(f,\theta_j\left(x_a,y_n\right)\right) \cdot g\left(f,\theta_j\left(x_a,y_m\right)\right) \cdot \mathrm{e}^{i\cdot k\cdot(|\mathbf{r}_{x_a,y_n}-\mathbf{r}_j|+|\mathbf{r}_{x_a,y_m}-\mathbf{r}_j|)} \right],$$

where $\mathbf{r}_{x_a,y_n} = \|x_a - \Delta x_{TR}/2, y_n, 0\|^T$ is the coordinate vector of the transmitting element n, $\mathbf{r}_{x_a,y_m} = \|x_a + \Delta x_{TR}/2, y_m, 0\|^T$ is the coordinate vector of the receiving element m, $k = 2\pi f/c$ is the wavenumber, $g(f, \theta)$ is the radiation pattern of the transmitting and receiving elements.

The processing of multi-static data to get microwave images of the modeled objects was performed through the back projection method [5], in which the complex value of the reconstructed image is given by:

$$\begin{aligned} E_R(x,y,z) \;=\; & \sum_{f=F_{\min}}^{F_{\max}} \sum_{x_a=0}^{\Delta x\cdot N_x} \sum_{n=1}^{N_T} \sum_{m=1}^{N_R} \Big[E(n,m,x_a,f) \\ & \times \exp\left(-i\cdot k\cdot\left(|\mathbf{r}_{x_a,y_n}-\mathbf{r}_{x,y,z}| + |\mathbf{r}_{x_a,y_m}-\mathbf{r}_{x,y,z}|\right)\right) \Big], \end{aligned}$$

where $\mathbf{r}_{x,y,z} = \|x, y, z\|^T$ is the coordinate vector of a point in space where the reconstructed image is calculated.

4. SIMULATION RESULTS

The comparison of the mono-static and multi-static methods was carried out on the model (Fig. 2(a)) of a gas pistol (Fig. 2(b)), reproduced in Autodesk 3DS Max.

At first, the radar signal samples of the pistol for mono-static and multi-static methods were simulated. The pistol was at the distance of 75 cm from the scan surface. The reconstruction was done for one frequency (10 GHz) and for the six frequencies evenly distributed in the range 10–16 GHz. The dimensions of the reconstructed images were 0.4 by 0.4 m. The results are shown in Figs. 3–4.

The second numerical experiment was done with the same pistol model on a human body model, Fig. 5. The distance to the object was 75 cm as in the experiments above.

The scan area, as well as the dimensions of reconstructed images, was 1.3 by 1.3 m. The results of reconstruction are shown in Figs. 6–7.

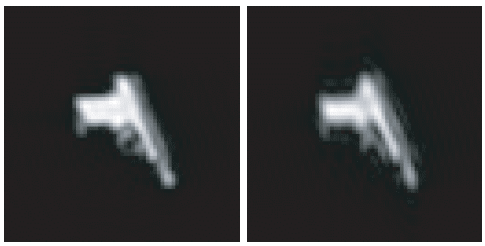

(a) (b)

Figure 3: Microwave image of the pistol reconstructed for a single-frequency. (a) Mono-static case, (b) multi-static case.

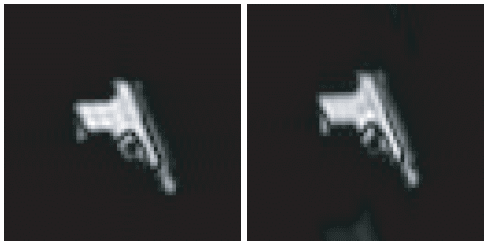

(a) (b)

Figure 4: Microwave image of the pistol reconstructed for a wide-band hologram. (a) Mono-static case. (b) multi-static case.

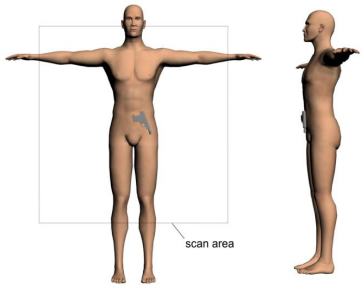

Figure 5: Human model with a pistol.

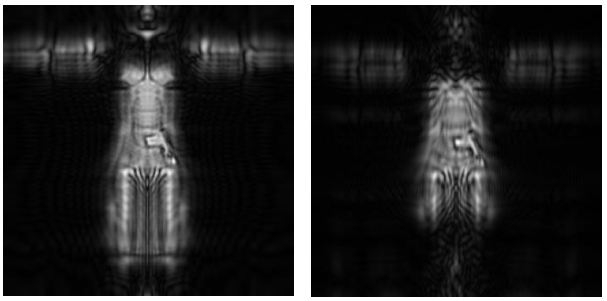

(a) (b)

Figure 6: Microwave images of the pistol and body reconstructed for a single-frequency. (a) Mono-static case, (b) multi-static case.

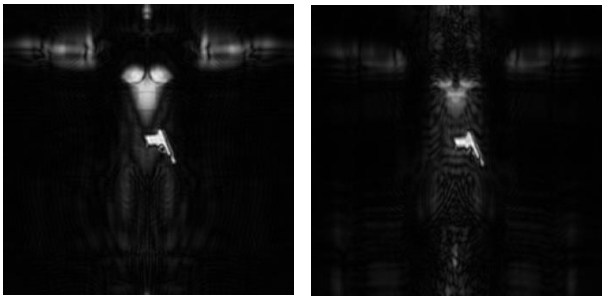

(a) (b)

Figure 7: Microwave images of the pistol and body reconstructed for a wide-band hologram. (a) Mono-static case, (b) multi-static case.

The above results show that the single-frequency methods are not suited for the complex objects such as the pistol and human body because these methods lack the range resolution. The reflection from the body surface (even though it is farther from the scan plane than the pistol) is superimposed on the reflection from the pistol and makes its recognition difficult in the reconstructed image. The pistol can be recognized, but one should remember that these results were obtained by numerical simulation. Most probably, in real experiments the results would be worse because of multiple reflections from clothing that were not considered here.

The wide-band method, having range resolution, gives much better results. In Fig. 7(a) (mono-static case) one can see that both the pistol and the fragment of the human chest fall within the same range resolution cell, because the chest is at the same distance from the scan plane as the pistol. These two objects can not be separated by their distances, but as they are spaced in XOY plane, the pistol can be easily recognized in the image. In the multi-static case, the wide-band method also has significant advantage over single-frequency one. The reconstructed image (Fig. 7(b)) has almost the same quality as the image obtained in mono-static case (Fig. 7(a)). The small differences in the regions of arms and legs are caused by additional range selection resulting from the bistatic electromagnetic field samples in the multi-static antenna.

5. CONCLUSION

As the result of theoretical comparative analysis of mono-static and multi-static synthetic aperture radar image reconstruction in the context of personnel surveillance, the following practical conclusions were made.

1. For an isolated object (pistol), both the mono-static and multi-static approaches demonstrate virtually the same high quality of the reconstructed images at a single-frequency as well as in the wide band 10–16 GHz. The scanning multi-static antenna configuration, composed of two linear transmitting and receiving antenna arrays, can be essentially sparse and can have the number of elements that is less by an order of magnitude. To suppress slight artifacts of diffractive nature, it is recommended to use closely-packed arrangement of elements in one of the antenna arrays (transmitting or receiving). The other array should be sparse to keep the vertical size of the aperture.

2. If a pistol or another object is placed on the human body, the single-frequency mono-static antenna array (130 transmitting and 130 receiving elements) and the single-frequency multi-static antenna array (sparse receiving antenna array with 16 elements and closely-packed transmitting antenna array with 8 elements) are comparable in terms of image quality. The reconstructed microwave image of the pistol does not have a significant contrast against the body because the single-frequency method does not provide the range resolution.

3. The contrast enhancement of the pistol over the background of the human body can be achieved by using a wide-band sounding signal. The range resolution of 2.5 cm is achieved with the bandwidth of 6 GHz. This bandwidth is wide enough to detect confidently the pistol over the body by contrast (see Fig. 7).

4. The main advantage of the multi-static antenna in comparison with mono-static one is the reduction of transceiver elements by an order of magnitude that leads to a lower cost of the radar system.

ACKNOWLEDGMENT

Support for this work was provided by the Ministry of Education and Science of the Russian Federation under project #8.1211.2014/K.

REFERENCES

1. Daniels, D. J., *EM Detection of Concealed Targets*, Wiley-IEEE Press, 2009.
2. Security & Detection Systems, "Advanced personnel screening," 2016, [Online]. Available: http://www.sds.l-3com.com/products/advancedimagingtech.htm.
3. Sheen, D. M. and T. E. Hall, "Reconstruction techniques for sparse multi-static linear array microwave imaging," D. A. Wikner and A. R. Luukanen, Eds., 90780I, Jun. 2014, [Online]. Available: http://proceedings.spiedigitallibrary.org/proceeding.aspx?doi=10.1117/12.2053814.
4. Razevig, V., S. Ivashov, I. Vasiliev, and A. Zhuravlev, "Comparison of different methods for reconstruction of microwave holograms recorded by the subsurface radar," *2012 14th International Conference on Ground Penetrating Radar (GPR)*, 331–335, Jun. 2012.
5. Kuriksha, A. A., "The reciprocal projection algorithm used for reconstructing a spatial distribution of wave sources," *Journal of Communications Technology and Electronics*, Vol. 47, No. 12, 1355–1360, 2002.
6. Chapurskii, V. V., "Receiving the radio-holographic images of objects on the basis of sparse MIMO-type antenna arrays with the single-frequency and multi-frequency radiations," Herald of the Bauman Moscow State Technical University, Series *Instrument Engineering*, Vol. 4, No. 85, 72–91, 2011.
7. Chapurskii, V. V., "Synthesis of microwave images of the objects with linear antenna array of MIMO type," *Herald of the Bauman Moscow State Technical University, Series Instrument Engineering*, No. Special Issue 7, 115–123, 2012.
8. Shtager, E., "Scattering microwaves from complex targets," *Radio and Communication*, Moscow, 1986.
9. Stutzman, W. L. and G. A. Thiele, *Antenna Theory and Design*, 2nd Edition, J. Wiley, USA, 1998.
10. Sheen, D. M., D. L. McMakin, and T. E. Hall, "Three-dimensional millimeter-wave imaging for concealed weapon detection," *IEEE Transactions on Microwave Theory and Techniques*, Vol. 49, No. 9, 1581–1592, Sep. 2001.